# Closure technique after carotid endarterectomy influences local hemodynamics

**Gareth J. Harrison, MBChB, MRCS,[a] Thien V. How, PhD,[b] Robert J. Poole, PhD,[c] John A. Brennan, MD,[a] Jagjeeth B. Naik, MD,[a] S. Rao Vallabhaneni, MD,[a]** and **Robert K. Fisher, MD,[a]**
*Liverpool, United Kingdom*

***Background:*** **Meta-analysis supports patch angioplasty after carotid endarterectomy (CEA); however, studies indicate considerable variation in practice. The hemodynamic effect of a patch is unclear and this study attempted to elucidate this and guide patch width selection.**
***Methods:*** **Four groups were selected: healthy volunteers and patients undergoing CEA with primary closure, trimmed patch (5 mm), or 8-mm patch angioplasty. Computer-generated three-dimensional models of carotid bifurcations were produced from transverse ultrasound images recorded at 1-mm intervals. Rapid prototyping generated models for flow visualization studies. Computational fluid dynamic studies were performed for each model and validated by flow visualization. Mean wall shear stress (WSS) and oscillatory shear index (OSI) maps were created for each model using pulsatile inflow at 300 mL/min. WSS of <0.4 Pa and OSI >0.3 were considered pathological, predisposing to accretion of intimal hyperplasia. The resultant WSS and OSI maps were compared.**
***Results:*** **The four groups comprised 8 normal carotid arteries, 6 primary closures, 6 trimmed patches, and seven 8-mm patches. Flow visualization identified flow separation and recirculation at the bifurcation increased with a patch and was related to the patch width. Computational fluid dynamic identified that primary closure had the fewest areas of low WSS or elevated OSI but did have mild common carotid artery stenoses at the proximal arteriotomy that caused turbulence. Trimmed patches had more regions of abnormal WSS and OSI at the bifurcation, but 8-mm patches had the largest areas of deleteriously low WSS and high OSI. Qualitative comparison among the four groups confirmed that incorporation of a patch increased areas of low WSS and high OSI at the bifurcation and that this was related to patch width.**
***Conclusions:*** **Closure technique after CEA influences the hemodynamic profile. Patching does not appear to generate favorable flow dynamics. However, a trimmed 5-mm patch may offer hemodynamic benefits over an 8-mm patch and may be the preferred option. (J Vasc Surg 2014;60:418-27.)**

After standard carotid endarterectomy (CEA), the arteriotomy may be closed primarily or by incorporating a patch. A recent meta-analysis suggested some benefit with patch angioplasty[1]; however, the clinical effects of different patch size have not been studied. A recent survey of vascular surgeons demonstrated that 65% routinely patch, and the remainder patch selectively according to the internal carotid artery (ICA) diameter.[2] Of the obligate patch users, 58% used the full patch width (median, 8 mm), 28% routinely trimmed (median, 6 mm), and 14% variably trimmed the patch (median, 7.5 mm). Patch composition included Dacron (DuPont, Wilmington, Del), polytetrafluoroethylene, and bovine pericardium, all of which were trimmed in some cases. Vein was rarely used. These survey results indicate three approximately equally sized patient groups: primary closure, trimmed patches, and full-size patches.

From The Regional Vascular Unit, Liverpool Royal Hospital[a]; and the Institute of Ageing and Chronic Disease[b] and the School of Engineering,[c] University of Liverpool.
Author conflict of interest: none.
Reprint requests: Gareth J. Harrison, MBChB, MRCS, Regional Vascular Unit, Royal Liverpool University Hospital, Prescot St, Liverpool L7 8XP, UK (e-mail: garethjamesharrison@yahoo.co.uk).
The editors and reviewers of this article have no relevant financial relationships to disclose per the JVS policy that requires reviewers to decline review of any manuscript for which they may have a conflict of interest.
0741-5214/$36.00

http://dx.doi.org/10.1016/j.jvs.2014.01.069

The carotid bifurcation in older adults has a complex and variable geometry, with three-dimensional (3D) structures and often an elliptical cross-section.[3,4] The complexity of the geometry influences the hemodynamics within the bifurcation, in contrast to hemodynamics in the common carotid vessel. Flow through a straight tube, such as the common carotid artery (CCA), is smoothly varying (laminar), unidirectional, and undisturbed. However, flow in the bifurcation is nonplanar and swirling effects ("helical flow") are important in modifying the distribution of wall shear stress (WSS).[5,6] Laminar flow up to the arterial division produces a velocity highest at the flow divider. Opposite to the divider, the velocity is lower, and the flow pattern is complicated by zones of recirculation and vortices[7] that result in complex WSS patterns. WSS is defined as a stress that is applied parallel to the vessel wall compared with normal stress that is applied perpendicular.[8] Areas of low WSS may predispose to intimal thickening and atherosclerosis.[9]

This study aimed to compare the influence of primary closure and patch angioplasty of 5-mm and 8-mm widths on the flow patterns and hemodynamic forces within an endarterectomized carotid artery.

## METHODS

This study was approved by the Regional Research Ethics Committee (REC reference 10/H1016/38).

**Table I.** Numbers of patients scanned and number of successful models in each group

| *Variable* | *Scans* | *8-mm patch* | *Successful model* | *5-mm patch* | *Successful model* | *Primary closure* | *Successful model* |
|---|---|---|---|---|---|---|---|
| Postoperative | 23 (12) | 11 (6) | 5 (2) | 6 (2) | 4 (1) | 6 (4) | 6 (4) |
| Intraoperative | 11 (6) | 8 (5) | 2 (1) | 3 (1) | 2 (1) | 0 | 0 |

Data presented are total number (number of females).

**Patient recruitment.** Two groups of patients were recruited. A postoperative group, consisting of consecutive patients undergoing CEA, was identified from the institution's entries into the United Kingdom (UK) National Vascular Database. Postoperative patients had a single ultrasound scan at between 5 and 13 months. The other group was recruited preoperatively to perform imaging perioperatively, upon completion of arteriotomy closure. Patients undergoing CEA for restenosis or radiation-induced stenosis were excluded. A control group of healthy volunteers was recruited to enable study of a normal carotid artery.

**CEA procedures.** All operations were standard CEA performed under general anesthetic. Shunt use was at the surgeon's discretion. Primary closure or patch angioplasty using 5-mm or 8-mm patches was determined by the surgeon's preference. An 8-mm-wide bovine pericardial patch (Vascu-Guard; Synovis Life Technologies, St. Paul, Minn) was used for all patched cases and trimmed to an appropriate length depending on the arteriotomy required. This commonly used patch[2] can be trimmed to ~5-mm wide by splitting the patch along its length, and this practice was adopted by one surgeon for all cases performed under his care. One surgeon preferred primary closure for all cases. In this series, therefore, ICA size did not influence closure technique. No record of perioperative events was made. All patients were discharged with antiplatelet medication and a statin.

**Ultrasound scan.** Scans were performed by three experienced vascular sonographers using a Philips iU22 ultrasound scanner (Philips Healthcare, DA Best, The Netherlands), with a 3- to 9-MHz (L9-3) linear array probe routinely used for carotid duplex imaging. The individual was positioned at 45° facing the contralateral direction. The probe was mounted in a specially designed rig to enable a transverse luminal image. The most cranial image of the ICA was recorded with subsequent images at 1-mm intervals caudally until at least 5-mm below the patch or 2-cm caudal to the bifurcation.

To manufacture a 3D model, the images were recorded at the same planar position to produce an accurate model and were also gated for the respiratory cycle to mitigate any movement artefact during 3D modelling. Respiratory gating was performed by detecting a rise in temperature through exhaled air using a temperature probe mounted within a facemask. The output from the temperature probe was connected to an oscilloscope which the sonographer used to trigger image acquisition.

**Modeling.** Options for developing a 3D reconstruction include ultrasound imaging, computed tomography angiography or magnetic resonance angiography. Although computed tomography angiography and magnetic resonance angiography are used in the preoperative clinical setting, there is no routine indication for these to be performed postoperatively. We therefore used ultrasound imaging because it avoids the risks of contrast and radiation exposure.

The method for reconstruction is well described.[10,11] The series of transverse ultrasound images of all patients were imported into Scan IP software (Simpleware, Exeter, UK), which is designed to convert them into 3D models. The lumen was manually traced on each image slice by the lead investigator. Because each slice was 1-mm apart, smoothing to a maximum of 1-mm was used to produce a realistic, virtual 3D model. These virtual 3D models were used to generate meshes for computational fluid dynamic (CFD) studies and to manufacture clear silicone rubber models for flow visualization studies.

Flow visualization studies were performed to investigate qualitatively flow patterns and their evolution through the cardiac cycle. The subsequent quantitative assessment of the flow and WSS was performed using CFDs. Comparison of flow visualization images with velocity vector plots from the same stage of the cardiac cycle allowed qualitative validation of the CFD results.

**Flow visualization.** Flow visualization studies were performed on one normal carotid model, three models of primary closures, and five models of each of the 5-mm and 8-mm patch angioplasties. These were selected to represent the average geometry observed across each group. A rapid prototyping technique was used to create clear, rigid, silicone models of the carotid bifurcations.[12] The models were incorporated into a flow rig reproducing the pulsatile blood flow observed in the CCA of a healthy volunteer. The pump output was recorded to identify the position within the cardiac cycle. Flow rates were monitored by two ultrasound flow meters to maintain a 300 mL/min inflow rate and a flow split of 70% ICA to 30% external carotid artery (ECA).[13] A blood analog was used comprising distilled water with 40% glycerol to which was added 75 μm nylon tracer particles (Rilsan Blue; Elf Atochem, Carrollton, Ky). Neutral buoyancy of the particles in the fluid was ensured by addition of sodium chloride at 7%. The dynamic viscosity of the solution was 0.0035 pascal-second (Pa•s) and was within the range of normal human whole blood.[14] In practice, this figure varies slightly with shear rate, because blood is a non-Newtonian fluid.[15]

The model was illuminated with a 0.5-mm-thick laser light sheet produced by a 15 mW helium-neon laser fitted with a Lasiris (StockerYale Canada Inc, Dollard-des-

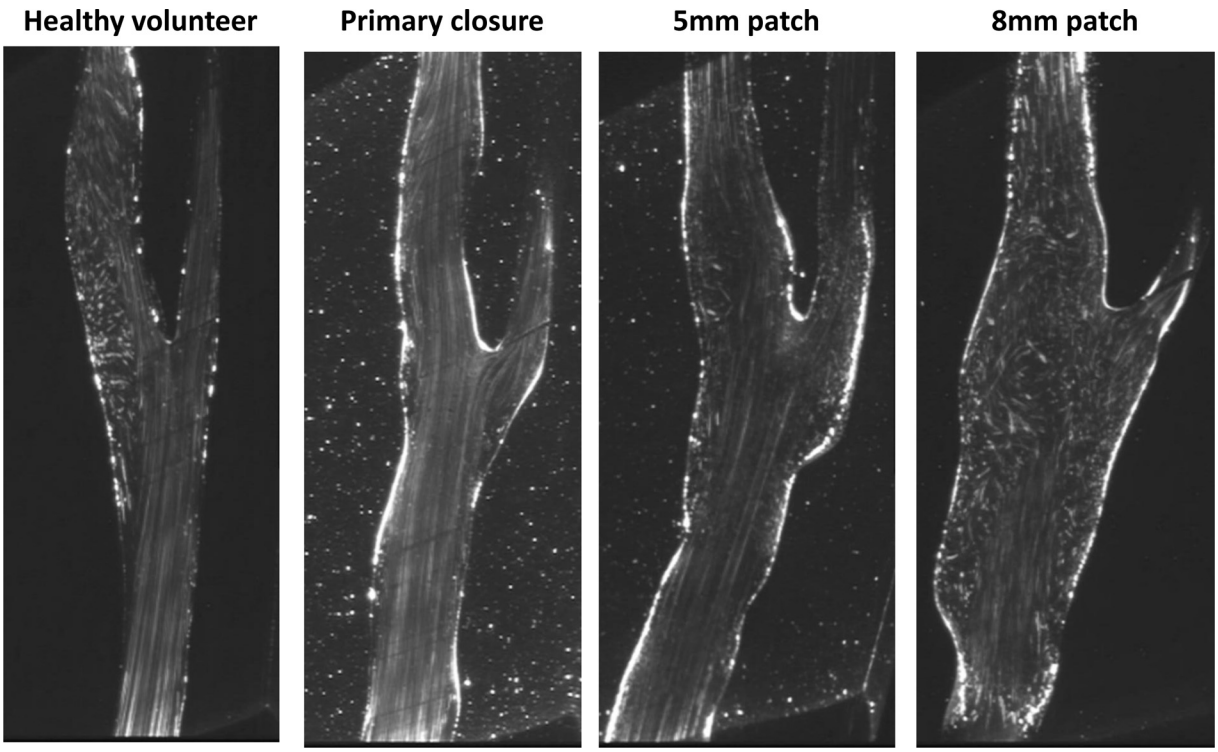


**Fig 1.** Flow visualization images during deceleration.

Ormeaux, QC, Canada) line generator in the anterior and lateral planes. The planar images were recorded with a video camera at 25 frames/s. With a pulse rate of 70 beats/min, this equated to 20 images per cardiac cycle. Each image frame was reviewed to identify features of flow separation or recirculation and their onset and decay during the cardiac cycle. This method has been reported previously.[16]

**CFD assessment.** CFD is a means of simulating real flow by solving the governing Navier-Stokes equations. These are essentially Newton's second law (force = mass × acceleration) but applied to a fluid element. To define the geometry, a volume mesh was constructed of 40,000 to 60,000 tetrahedra using Gambit software (Ansys UK Ltd, Sheffield, UK) with the virtual 3D models. Cylindrical extensions, chosen to be 50 mm in length to ensure a minimum of three times the diameter of the largest CCA, were added to minimize flow disturbance artifact at the inlets. The CFD program used was Fluent 6.2 (Ansys UK Ltd). WSS was determined from the velocity field, which the CFD software could output directly. This technique is well recognized.[17]

The fluid was assumed to have a density of 1050 kg/m$^3$ and viscosity of 0.0035 Pa•s (ie, similar to that of the fluid used for flow visualization studies). The CCA was selected as the velocity inlet, and ECA (weighting 0.3) and ICA (weighting 0.7) were selected as outflows. The walls of the models were assumed to be rigid. Each model was solved using steady flow of 30 cm/s into the CCA to produce an initial solution. The solution was deemed to have converged when the residual error reached $1 \times 10^{-6}$.

**Table II.** Percentage of cardiac cycle displaying flow disturbance by model

| *Model* | *No.* | *Proportion of cardiac cycle with flow separation, median % (range)* |
|---|---|---|
| Normal | 1 | 40 |
| Primary closure | 3 | 40 (20-85) |
| 5-mm patch | 5 | 55 (45-70) |
| 8-mm patch | 5 | 70 (55-75) |

For pulsatile flow simulation, the CCA waveform from a healthy volunteer was recorded. The best match curve of a combination of polynomial equations was obtained, up to sixth order, in five sections. Because the resulting graph was created in arbitrary units, a correction factor was applied to the formula. This procedure used the cross-sectional area of the CCA extension of each model to apply the correct velocity for a flow input of 300 mL/min.

The pulsatile flow simulation used 100 time steps per cardiac cycle and 5000 iterations per time step. One whole cardiac cycle was allowed to converge, before results were taken in the second cycle, to minimize any numeric artifact. Data were presented at every five time steps.

The results of CFD calculations were presented using Tecplot 9.0 software (Tecplot Inc, Bellevue, Wash).

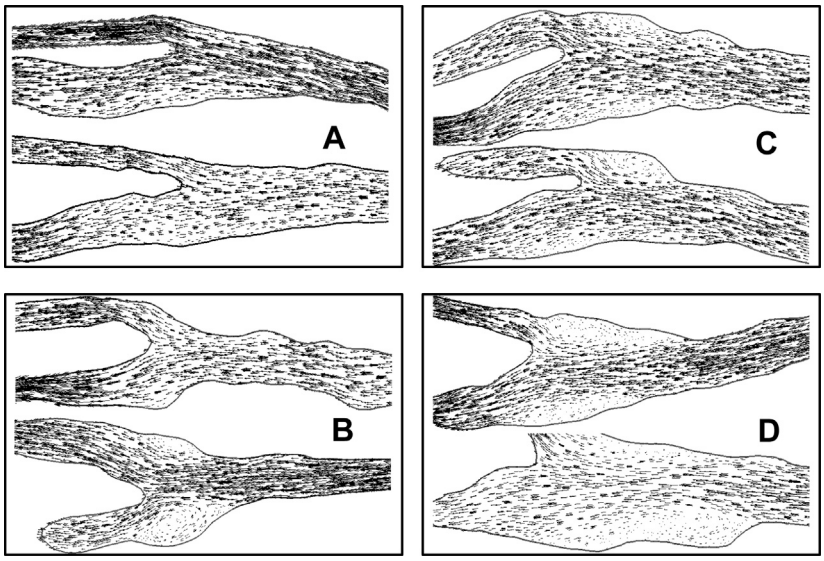


**Fig 2.** Velocity vector images through the carotid bulb of **(A)** normal bifurcations, **(B)** primary closures, **(C)** 5-mm patch angioplasty, and **(D)** 8-mm patch angioplasty during the deceleration phase of systole.

Time-averaged WSS data were displayed within the range of 0 to 1 Pa to show the low extremes of WSS because values of <0.4 Pa have been demonstrated to be detrimental.[9] This software was also used to produce maps of oscillatory shear index (OSI), which defines the proportion of the cardiac cycle in which flow was antegrade, thereby offering a measure of recirculation. An OSI of 0 represents antegrade flow throughout the cycle, and an OSI of 1.0 signifies retrograde flow throughout the cycle. An OSI >0.3 has been suggested to represent disordered flow in which the direction of the shear stress alternates frequently and has been associated with the development of intimal hyperplasia and atherosclerosis.

Statistical analysis of CFD data was limited, considering the variation in size of each model and the number and size of mesh elements. WSS and OSI figures were recorded at the origin of the ICA and at 10-mm proximal to the origin of the ICA. Statistical comparison was made with box-and-whisker plots.

## RESULTS

Nine healthy volunteers between the ages of 25 and 44 were recruited to define normal geometry and hemodynamics, and 34 patients (16 men) were recruited for carotid scanning, 11 of whom had scans intraoperatively and 23 postoperatively. The median patient age was 70 years (range, 53-87 years). The CEA was left-sided in 16 patients. In the postoperative group, scanning was performed at a median of 11 months (range, 5-13 months) after surgery. No postoperative strokes, thromboses, or significant stenoses were identified. Routine long-term follow-up was not undertaken.

From these 43 individuals, 19 patient models (56%) and 8 volunteer models (89%) were suitable for full CFD analysis. Reasons for failure of model generation were poor image quality or high bifurcation that resulted in inadequate capture of the ICA in eight patients and one volunteer. Excessive patient movement prevented 3D model construction for four postoperative patients. Two sets of images had no view of the ECA origin, and one set failed to include the proximal limit of the patch. The final number in each of the study groups is summarized in Table I.

### Flow visualization

**Normal.** Flow visualization images during the acceleration phase of systole demonstrated the greatest flow velocity within the center of the bulb near to the flow divider (Fig 1). Opposite the flow divider, flow velocity appeared lower on both lateral walls of the bulb. At the peak of systole, a very similar pattern of apparently laminar flow was visualized, although the velocity was considerably greater.

During the deceleration phase of systole, the area of low velocity flow within the bulb and opposite the flow divider developed into an area of flow separation, most clearly defined on the anterior image. A similar pattern was seen during diastole. Table II indicates the number of frames that feature flow separation.

**Primary closure.** Three models underwent flow visualization, two of which displayed the usual geometric features of primary closure, with minimal expansion of the bulb. In the first model, there was flow separation or recirculation in 20% of the cardiac cycle (Table II), occupying a limited region of the bulb during deceleration. This flow structure was centered within a region of poststenotic dilatation immediately distal to the limit of the endarterectomy within the CCA. The second model had similar features in a comparable position. Flow separation within the third model was seen opposite the flow divider on both lateral walls during systole and diastole. This third model

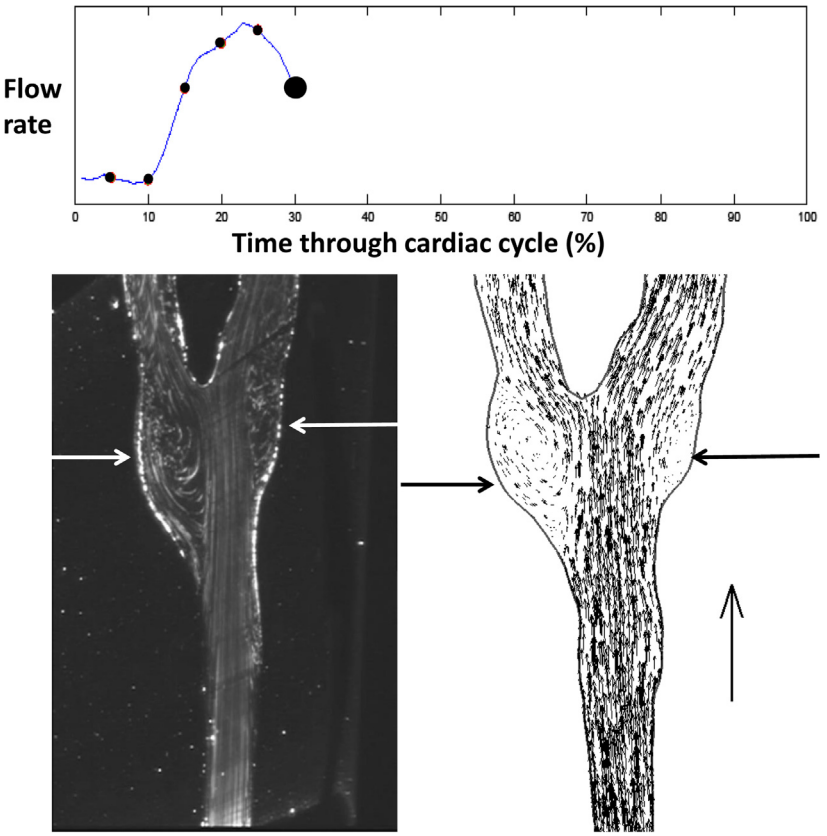


**Fig 3.** Example image compares flow visualization and computational fluid dynamic (CFD) velocity vector plot during deceleration, used to validate CFD. The *arrows* identify similar regions of flow separation.

had more pronounced stenosis and poststenotic dilatation at the proximal limit of the endarterectomy.

**Angioplasty with 5-mm patch.** Unidirectional flow, with greatest velocity in the center of the lumen, was identified throughout the carotid bulb during acceleration. During deceleration, the lateral walls of the bulb demonstrated regions of flow separation/rudimentary recirculation. In diastole, flow separation was found at the lateral margin of the ICA bulb, opposite to the flow divider, and flow deviated around this area of separation.

**Angioplasty with 8-mm patch.** Flow separation was seen during acceleration at the lateral margins of the bulb in all three models. At the peak of systole, laminar flow was visualized throughout the CCA and the center of the bulb, and ICA with flow separation and recirculation was seen opposite the flow divider. During deceleration, flow separation was noted at both lateral margins of the bulb. Diastolic flow continued to show these features, although the velocity magnitude was lower. The proportion of the cardiac cycle with features of flow separation is summarized in Table II.

## Validation of CFD

CFD was performed on all models, and the velocity vectors were calculated. Fig 2 shows velocity vectors in a coronal section for two representative examples of each model type. Qualitative comparisons of flow visualization images with the CFD velocity vector plots in the same plane of the model were performed at the acceleration, peak, and deceleration phases of systole and diastole in all 14 models that underwent flow visualization. The position of areas of flow separation and recirculation corresponded very closely, offering qualitative validation of the CFD methodology. Fig 3 illustrates an example image in which similar areas of flow separation are seen opposite the flow divider at the lateral walls with both flow visualization and CFD vector images.

## CFD assessments

**Normal carotid.** Fig 4 shows the mean WSS (ie, averaged over the cardiac cycle) and Fig 5 represents the OSI in all carotid bifurcations. The value of mean WSS varied between participants within this group: three of eight displayed extensive areas of darker blue coloring, indicating shear stress <0.2 Pa, four had small regions of WSS below 0.3 Pa, which did not occupy the whole circumference of the vessel, and one had no areas of WSS <0.4 Pa. These variations were reflected in the OSI plots. Five models showed regions >0.3, one of which had a peak of 0.7.

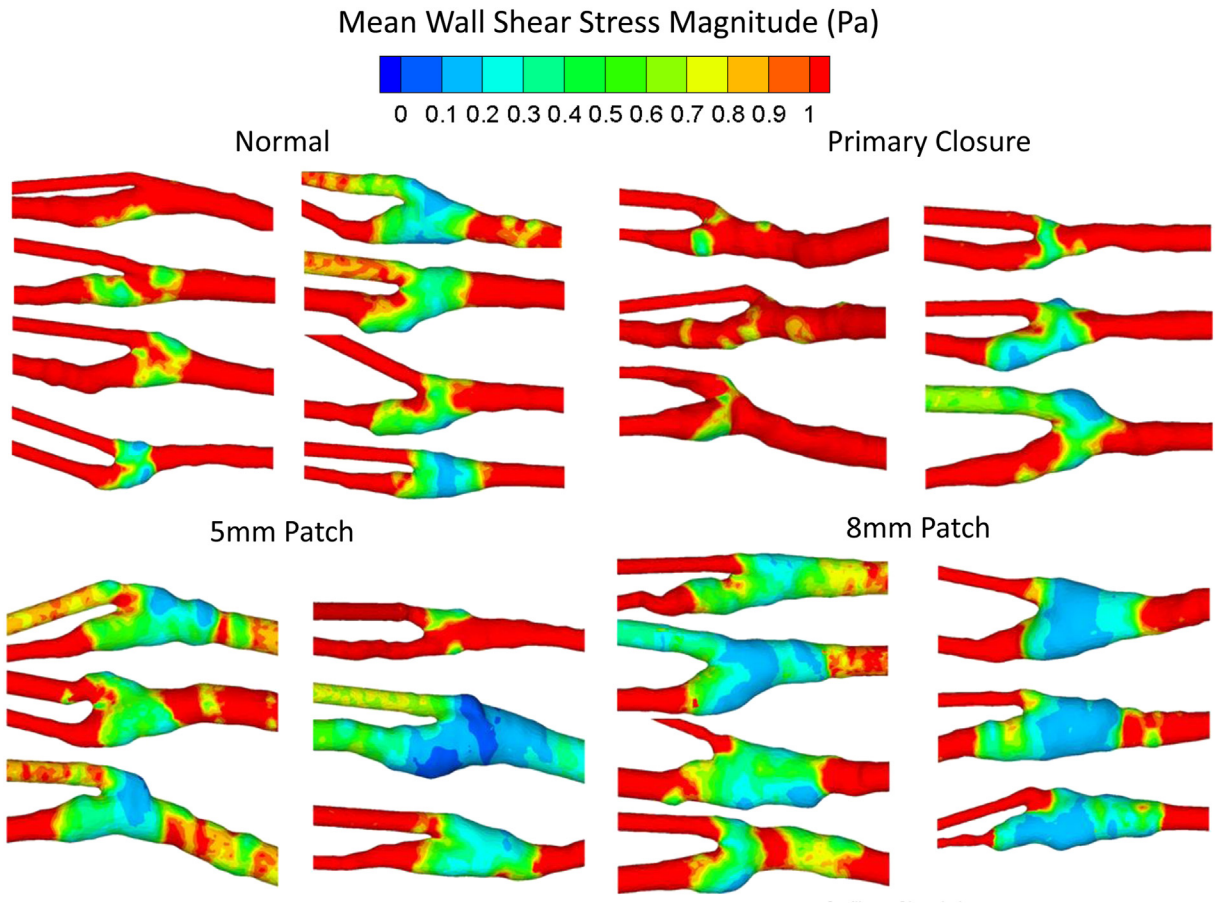


**Fig 4.** Wall shear stress (WSS) for normal carotids and all types of reconstruction.

**Primary closures.** Four of six models displayed areas of low WSS, two had small areas, and two had more extensive WSS <0.4 Pa but did not occupy the full circumference of the artery (Fig 4). One of these had an elevated OSI >0.5 and the other >0.8 (Fig 5). These two models demonstrated poststenotic dilatation at the proximal endarterectomy site.

**Angioplasty with 5-mm patch.** The six 5-mm patch angioplasty models had some areas of mean WSS <0.4 Pa (Fig 4). Two models had very limited areas of WSS <0.4 Pa, three had regions <0.2 Pa, which was not circumferential, and one model had WSS <0.1 Pa that featured through the full circumference of the vessel. This atypical model was particularly large in diameter. In addition, the WSS was 0.5 Pa in the more distal ICA compared with >1 Pa in all other models. The OSI reached >0.3 in four of six models, with small areas reaching >0.8 in three models (Fig 5).

**Angioplasty with 8-mm patch.** All seven 8-mm patch angioplasty models displayed WSS of <0.4 Pa occupying the full vessel circumference (Fig 5). In addition all seven models had at least some small areas of WSS <0.2 Pa, which was circumferential in four models. The OSI was >0.5 in six of seven models and was circumferential in two of them (Fig 6). In addition, a specific area of OSI >0.8 was noted at a dilated region within the patch in two models.

Although regions of very low WSS were seen in all groups, the primary closures had the fewest areas of mean WSS <0.4 Pa. The extent of very low WSS was substantially greater in the 8-mm patch angioplasty group, with WSS in the range of 0.1 to 0.2 Pa occupying the full circumference of all vessels. Such areas were noted within the 5-mm patch angioplasty group but were less extensive and not circumferential. Table III reports the median lowest WSS and highest OSI at the ICA origin and 10-mm proximal to the bifurcation in the CCA. The lowest circumferential WSS and highest circumferential OSI at any point through the carotid bifurcation are displayed in Fig 6 as a box-and-whisker plot. Sex, time after surgery, and carotid size did not subjectively appear to affect CFD results, with the exception of the particularly large 5-mm patch model described above.

## DISCUSSION

This study demonstrates that different closure techniques after CEA alter the geometry and influence flow

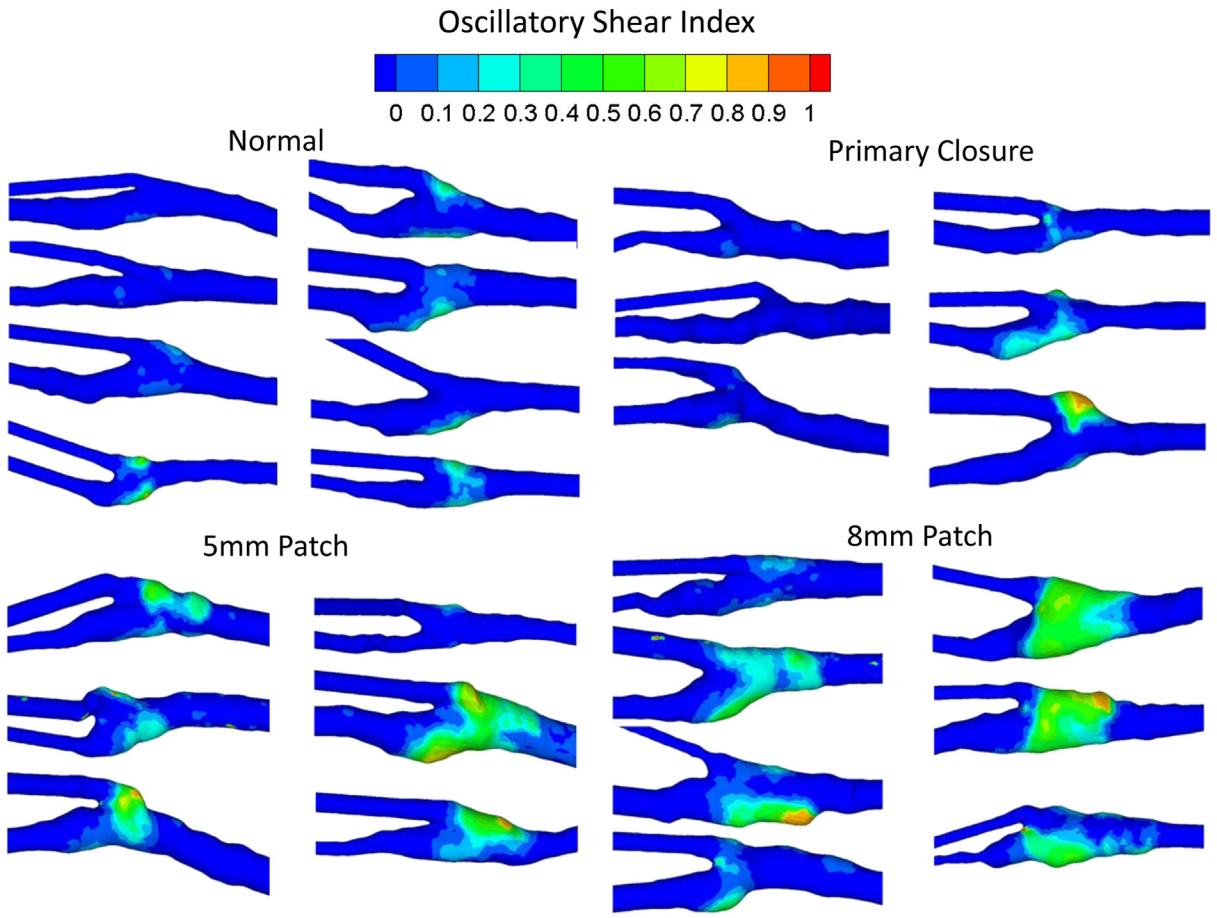


**Fig 5.** Oscillatory shear index (OSI) for normal carotids and all types of reconstruction.

and hemodynamics within the reconstructed vessel. This may, in turn, influence the behavior and remodelling of the vessel, potentially affecting clinical outcome.

Although clinical evidence would support patching,[1] this study suggests that the benefit is probably not attributable to optimization of hemodynamic forces. Some of the primary closure models produced flow patterns similar to the normal carotid models, which displayed more favorable hemodynamic patterns than the 5-mm and 8-mm patched reconstructions. However, there were also instances where the primary closure generated CCA stenosis at the caudal endarterectomy limit, resulting in deleterious hemodynamics. One may anticipate that these carotid arteries would be susceptible to intimal hyperplasia and would be at risk of critical stenosis and occlusion because of the limited volume of an already narrowed vessel.

Within the patched models, 5-mm and 8-mm patch angioplasty both demonstrated less advantageous hemodynamic profiles compared with the cohort of normal bifurcations. This was due to the altered geometry and was particularly pronounced for the 8-mm patch group, in which flow visualization displayed flow separation in 60% to 80% of the cardiac cycle in all models. All of the 8-mm models had extensive regions of low WSS, many of which were circumferential, which may potentiate the development of intimal hyperplasia. The benefit of patching may primarily be due to the increased volume of the reconstructed carotid bulb, which is better able to accommodate any neointimal hyperplasia. In addition, incorporating a patch may reduce technical error.

The meta-analysis comparing outcomes between primary closure and patching demonstrated an odds ratio for ipsilateral perioperative stroke of 0.31.[1] However, trials within the meta-analysis were variable.[18-20] The results of this study would suggest that if the clinical benefits of a patch are to be maintained, then a 5-mm patch may offer the more desirable hemodynamic profile while maintaining the physical attributes mentioned. The recent study suggesting that many surgeons use larger patches (8-mm median width)[2] indicates that a change to the narrower patch may be recommended, thereby harnessing the physical and technical benefits while minimizing deleterious hemodynamic forces.

Intuitively, patching an artery increases the cross-sectional area, resulting in lower WSSs, which this study corroborated. However, the geometric modification of

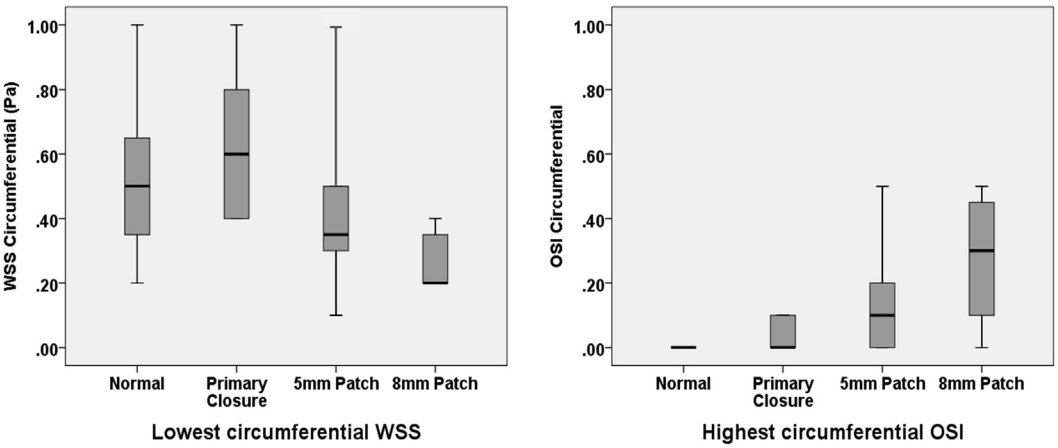


**Fig 6.** Box-and-whisker plot shows **(left)** lowest circumferential wall sheer stress (*WSS*) and **(right)** highest circumferential oscillatory shear index (*OSI*) within the carotid bifurcation. The *horizontal line* in the middle of each box indicates the median; the *top* and *bottom borders* of the box mark the 75th and 25th percentiles, respectively, and the *whiskers* mark the 90th and 10th percentiles.

**Table III.** Lowest wall sheer stress (*WSS*) and highest oscillatory shear index (*OSI*) at internal carotid artery (*ICA*) origin and common carotid artery (*CCA*)

| | *Lowest WSS* | | *Highest OSI* | |
|---|---|---|---|---|
| | *ICA origin* | *CCA* | *ICA origin* | *CCA* |
| *Model* | *Median (range)* | *Median (range)* | *Median (range)* | *Median (range)* |
| Normal | 0.4 (0.2-0.7) | 0.35 (0.2-1) | 0.1 (0-0.3) | 0.2 (0-0.7) |
| Primary closure | 0.5 (0.3-0.7) | 0.7 (0.3-1) | 0.1 (0-0.3) | 0.05 (0-0.5) |
| 5-mm patch | 0.45 (0.1-1) | 0.25 (0.2-0.5) | 0.15 (0-0.7) | 0.35 (0.2-0.7) |
| 8-mm patch | 0.3 (0.2-0.5) | 0.2 (0.2-0.5) | 0.4 (0.1-0.6) | 0.5 (0.1-0.7) |

the vessel by the patch also creates areas of flow separation and recirculation, as demonstrated by the flow visualization and velocity vector plots.

In addition to lowering WSS, these flow structures also contribute to the raised OSI, which is associated with the accretion of neointimal hyperplasia.[21] High OSI and low WSS are inextricably linked, because a region of a vessel that has extensive retrograde flow though the cardiac cycle will inevitably have low mean WSS throughout the entire cardiac cycle. The exact mechanism dictating the pathologic effects of low WSS is unclear but appears to be endothelial-cell related.[9,22-24]

This study indicates that the 5-mm patch reduces the area and duration of flow separation within the carotid bulb compared with the larger 8-mm model. In addition, it may be anticipated that areas of flow recirculation and separation increase the platelet residence time, which may predispose the deposition of thrombus and increase the risk of postoperative embolization and stroke. Despite such flow phenomena being observed within the patched vessels, the clinical data would not support this supposition, and no clinical outcome data exist with patches of different widths.[1]

Previous studies have compared the hemodynamics of primary closure with patch angioplasty. Archie and colleagues[25-28] used CFD to determine the velocities and WSS on simplified theoretical carotid bifurcation geometries designed to replicate a primarily closed CEA, a patch-reconstructed CEA, and an idealized smoothly tapered carotid artery bifurcation. Their results show that areas with significant geometric change produced extremes in shear stress, as confirmed by the present study. They recommended an optimal reconstruction with no bulb and avoidance of acute diameter changes, as seen with large patches. Their use of purely theoretic models, however, detracts from the applicability of the results. The in vivo geometry and flow parameters used in this current study offer more relevant information and also describe a reduction in deleterious flow structures within the narrow 5-mm patch compared with the 8-mm patch. Previous studies have identified healthy volunteers with pathologic WSS levels similar to the normal group in this study.[3]

The current study attempted to optimize the modelling and flow parameters but still has several limitations. Because the models are of different sizes, shapes, mesh density, and element size, only limited quantitative analysis

of the WSS and OSI maps could be performed. The lack of clear separation in the box-and-whisker plots between the 5-mm and 8-mm patches is likely to be a type 2 error.

The CFD analysis and the flow visualization experiments assumed that blood is a Newtonian fluid and ignored its non-Newtonian behavior. The vessel wall was also assumed to be noncompliant. These conditions, however, were not considered likely to have a significant effect on the hemodynamic forces.

Further study limitations include the relatively small number of participants, precluding meaningful statistical analysis, and the nonrandomized nature of the groups. Data from a number of patients could not be used, largely due to difficulty in accessing the more distal ICA intraoperatively. However, alternative methods of imaging were not considered practical or ethical. Only one flow rate was used to enable comparison of the effect of geometry on hemodynamics; thus, the flow rate was not patient-specific, but the geometry was.

Extrapolation of these results to other synthetic patches may not be accurate, but similar results with Dacron or polytetrafluoroethylene (both noncompliant) would be anticipated. These results are not applicable when considering the heterogeneity of size and compliance of vein patches. Caution must also be given when interpreting these results because other factors, such as native vessel geometry and surgical technique, may also affect the geometry of the reconstructed carotid bulb.

Future research involving randomization for patch size, although attractive, may be prohibitive, because a power calculation performed as part of the meta-analysis comparing primary closure and patch angioplasty suggested a cohort of 3000 patients.[1] A more practical option would be to record data on patch size within national registries. Any correlation of patch width and perioperative stroke or restenosis might support the findings presented that narrow patches confer some benefit over wider patches.

## CONCLUSIONS

Closure of the artery after CEA influences local flow velocity patterns and hemodynamic forces. Deleterious changes in WSS and OSI are observed with all closure techniques but are accentuated with increasing patch width. A single patch size cannot be recommended due to variation in carotid morphology; however, the results of this study suggest that the surgeon should try to avoid excessive dilatation of the vessel after reconstruction.

## AUTHOR CONTRIBUTIONS

Conception and design: GH, TH, RP, JB, JN, SV, RF
Analysis and interpretation: GH, TH, RP, RF
Data collection: GH
Writing the article: GH, TH, RP, RF
Critical revision of the article: GH, TH, RP, JB, JN, SV, RF
Final approval of the article: GH, TH, RP, JB, JN, SV, RF
Statistical analysis: GH, TH, RP, RF
Obtained funding: GH, TH, RP, RF
Overall responsibility: GH

## REFERENCES

1. Rerkasem K, Rothwell PM. Patch angioplasty versus primary closure for carotid endarterectomy. Cochrane Database Syst Rev 2009: CD000160.
2. Harrison G, Brennan J, Naik J, Vallabhaneni S, Fisher R. Patch variability following carotid endarterectomy: a survey of Great Britain and Ireland. Ann R Coll Surg Engl 2012;94:411-5.
3. Thomas JB, Antiga L, Che SL, Milner JS, Steinman DA, Spence JD, et al. Variation in the carotid bifurcation geometry of young versus older adults: implications for geometric risk of atherosclerosis. Stroke 2005;36:2450-6.
4. Goubergrits L, Affeld K, Fernandez-Britto J, Falcon L. Geometry of the human common carotid artery. A vessel cast study of 86 specimens. Pathol Res Pract 2002;198:543-51.
5. Sherwin SJ, Shah O, Doorly DJ, Peiró J, Papaharilaou Y, Watkins N, et al. The influence of out-of-plane geometry on the flow within a distal end-to-side anastomosis. J Biomech Eng 2000;122:86-95.
6. Papaharilaou Y, Doorly DJ, Sherwin SJ. The influence of out-of-plane geometry on pulsatile flow within a distal end-to-side anastomosis. J Biomech Eng 2002;35:1225-39.
7. Glagov S, Zarins C, Giddens DP, Ku DN. Hemodynamics and atherosclerosis. Insights and perspectives gained from studies of human arteries. Arch Pathol Lab Med 1988;112:1018-31.
8. Goldsmith HL, Turitto VT. Rheological aspects of thrombosis and haemostasis: basic principles and applications. ICTH-Report—Subcommittee on Rheology of the International Committee on Thrombosis and Haemostasis. Thromb Haemost 1986;55:415-35.
9. Malek AM, Alper SL, Izumo S. Hemodynamic shear stress and its role in atherosclerosis. JAMA 1999;282:2035-42.
10. Starmans-Kool MJ, Stanton AV, Zhao S, Xu XY, Thom SA, Hughes AD. Measurement of hemodynamics in human carotid artery using ultrasound and computational fluid dynamics. J Appl Physiol 2002;92: 957-61.
11. Hammer S, Jeays A, Allan PL, Hose R, Barber D, Easson WJ, et al. Acquisition of 3-D arterial geometries and integration with computational fluid dynamics. Ultrasound Med Biol 2009;35:2069-83.
12. Chong CK, Rowe CS, Sivanesan S, Rattray A, Black RA, Shortland AP, et al. Computer aided design and fabrication of models for in vitro studies of vascular fluid dynamics. Proc Inst Mech Eng H 1999;213:1-4.
13. Marshall I, Papathanasopoulou P, Wartolowska K. Carotid flow rates and flow division at the bifurcation in healthy volunteers. Physiol Meas 2004;25:691-7.
14. Lowe GD, Lee AJ, Rumley A, Price JF, Fowkes FG. Blood viscosity and risk of cardiovascular events: the Edinburgh Artery Study. Br J Haematol 1997;96:168-73.
15. Cokelet GR, Meiselman HJ. Macro- and micro-rheological properties of blood. In: Baskurt OK, Hardeman MR, Rampling MW, Meiselman HJ, editors. Handbook of hemorheology and hemodynamics. Amsterdam: IOS Press; 2007. p. 45-71.
16. Fisher RK, How TV, Carpenter T, Brennan JA, Harris PL. Optimising miller cuff dimensions: the influence of geometry on anastomotic flow patterns. Eur J Vasc Endovasc Surg 2001;21:251-60.
17. Nordgaard H, Swillens A, Nordhaug D, Kirkeby-Garstad I, Van Loo D, Vitale N. Impact of competitive flow on wall shear stress in coronary surgery: computational fluid dynamics of a LIMA-LAD model. Cardiovasc Res 2010;88:512-9.
18. Eikelboom BC, Ackerstaff RG, Hoeneveld H, Ludwig JW, Teeuwen C, Vermeulen FE, et al. Benefits of carotid patching: a randomized study. J Vasc Surg 1988;7:240-7.
19. Al-Rawi PG, Turner CL, Waran V, Ng I, Kirkpatrick PJ. A randomized trial of synthetic patch versus direct primary closure in carotid endarterectomy. Neurosurgery 2006;59:822-9.
20. AbuRahma AF, Robinson PA, Saiedy S, Kahn JH, Boland JP. Prospective randomized trial of carotid endarterectomy with primary closure and patch angioplasty with saphenous vein, jugular vein, and

polytetrafluoroethylene: long-term follow-up. J Vasc Surg 1998;27:222-32.
21. Ding Z, Wang K, Li J, Cong X. Flow field and oscillatory shear stress in a tuning-fork-shaped model of the average human carotid bifurcation. J Biomech 2001;34:1555-62.
22. Kuo L, Davis MJ, Chilian WM. Endothelium-dependent, flow-induced dilation of isolated coronary arterioles. Am J Physiol 1990;259:H1063-70.
23. Sharefkin JB, Diamond SL, Eskin SG, McIntyre LV, Dieffenbach CW. Fluid flow decreases preproendothelin mRNA levels and suppresses endothelin-1 peptide release in cultured human endothelial cells. J Vasc Surg 1991;14:1-9.
24. Zarins CK, Giddens DP, Bharadvaj BK, Sotturai VS, Mabon RF, Glagov S. Carotid bifurcation atherosclerosis. Quantitative correlation of plaque localization with flow velocity profiles and wall shear stress. Circ Res 1983;53:502-14.
25. Wells DR, Archie JP Jr, Kleinstreuer C. Effect of carotid artery geometry on the magnitude and distribution of wall shear stress gradients. J Vasc Surg 1996;23:667-78.
26. Hyun S, Kleinstreuer C, Archie JP Jr. Hemodynamics analyses of arterial expansions with implications to thrombosis and restenosis. Med Eng Phys 2000;22:13-27.
27. Hyun S, Kleinstreuer C, Archie JP Jr. Computer simulation and geometric design of endarterectomized carotid artery bifurcations. Crit Rev Biomed Eng 2000;28:53-9.
28. Hyun S, Kleinstreuer C, Archie JP Jr. Computational particle-hemodynamics analysis and geometric reconstruction after carotid endarterectomy. Comput Biol Med 2001;31:365-84.

Submitted Nov 14, 2013; accepted Jan 30, 2014.